DESIGN WORK OF THE ERL-FEL AS THE HIGH INTENSE EUV LIGHT SOURCE *

N. Nakamura, S. Chen, T. Furuya, K. Haga, I. Hanyu, K. Harada, T. Honda, Y. Honda, E. Kako, Y. Kamiya, R. Kato, H. Kawata, Y. Kobayashi, T. Konomi, T. Kubo, S. Michizono, T. Miyajima, H. Nakai, T. Obina, K. Oide, H. Sakai, S. Sakanaka, M. Shimada, K. Tsuchiya, K. Umemori, M. Yamamoto,
KEK, Oho, Tsukuba, Ibaraki 305-0801, Japan
R. Hajima, N. Nishimori, JAEA, Tokai, Naka, Ibaraki 319-1195, Japan

Abstract

Energy recovery linac(ERL) based free electron lasers(FELs) are promising candidates of high-power EUV sources for lithography. We have designed a 10-kW class ERL-FEL operated at 13.5 nm and demonstrated the FEL power of more than 10 kW at the average current of less than 10 mA by using simulations. In this paper, we will present the design work of the ERL-FEL as the high-power EUV source.

INTRODUCTION

High-power EUV sources are required in the future for lithography. EUV FELs are becoming candidates of the EUV sources because the order of EUV-FEL size and cost can be acceptable. ERL-based FELs have merits of energy recovery, low dumped beam power and activation compared with those based on ordinary linear accelerators. We recently started the design study on the ERL-based FEL as a high intense EUV source for lithography applications. In this design work, the first target is 10-kW FEL power at 13.5 nm and the beam energy is fixed to 800 MeV. For the design, we use available technology without too much development and make the most of resources of the Compact ERL(cERL) at KEK[1].

INJECTOR DESIGN

Figure 1 shows layout of the injector system designed for the EUV source. The DC photocathode gun has the same structure of the 2nd gun developed at the cERL[2]. It succeeded in the HV conditioning up to 550 kV and 50-hour holding test of 500 kV. Two solenoid magnets and one buncher cavity are used like in the cERL injector. Two cERL injector cryomodules with six 2-cell superconducting (SC) cavities are used to increase the injection beam energy up to 10.511 MeV. A merger system is newly designed.

Injector parameters are optimized before the merger by using *GPT*[3] tracking and genetic algorithm. Figure 2 shows an example of the optimized normalized emittance and momentum spread as a function of bunch length for the bunch charge of 60pC. Taking account of the optimization results before the merger and transverse emittance growth due to the merger, we estimate the injector parameter values at the merger exit. The estimated parameter values are summarized in Table 1. These values are used as the initial parameter values for simulations including the bunch compression.

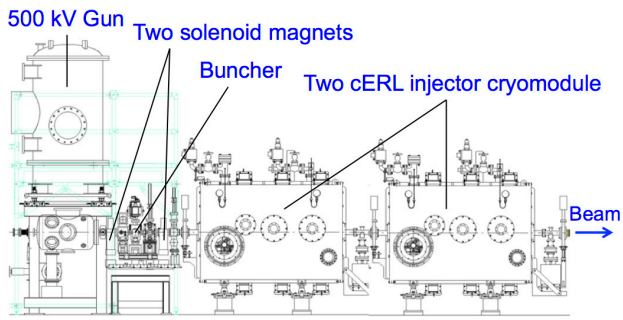

Figure 1: Layout of the injector system designed for the EUV source. The merger system is not included.

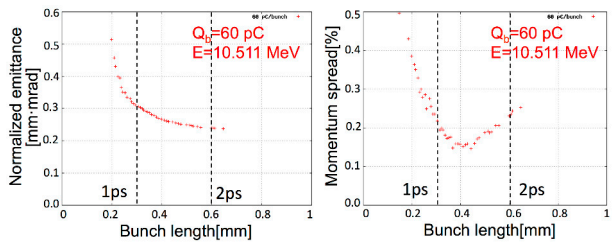

Figure 2: Optimized normalized emittance (left) and momentum spread (right) as a function of the bunch length at the bunch charge of 60 pC for the designed injector system before the merger.

Table 1: Estimated Injector Parameter Values at the Merger Exit

Bunch charge	σ_t * [ps]	ε_n # (ε_{nx}=ε_{ny}) [mm·mrad]	σ_p/p † [%]
60 pC	1	0.60	0.25
60 pC	2	0.55	0.25
100 pC	1	0.80	0.35
100 pC	2	0.60	0.16

* Bunch length # Normalized emittance † Momentum spread

*norio.nakamura@kek.jp

ISBN 978-3-95450-183-0

MAIN LINAC DESIGN

Cavity Design

The cERL main-linac cavities, called Model 2, are stably operated at about 8.5MV/m[4]. However the field emission of the cavities becomes significant above about 10 MV/m. Therefore we will use a different design called Model 1 for the EUV source. The Model-1 cavity[5] illustrated in Fig. 3 is a Tesla-type 9-cell cavity with a large-aperture HOM-damped beam pipe. This cavity has a smaller ratio of the peak to acceleration electric field as compared to Model 2. Therefore stable operation at 12.5 MV/m seems achievable. The detailed structure of the Model-1 cavity is under design and the large-aperture HOM-damped beam pipe may be applied to the other side.

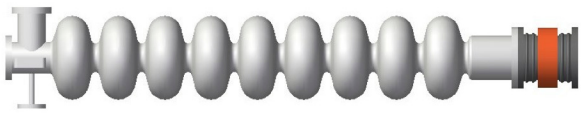

Figure 3: Illustration of the Model-1 cavity.

Table 2: Comparison of Model 1 and Model 2

	Model 1	**Model 2**
Frequency	1.3 GHz	1.3 GHz
R_{sh}/Q	1007 Ω	897 Ω
E_p/E_{acc}	2.0	3.0
Iris diameter	70 mm	80 mm

Main Linac Optics

The main linac has 64 cavities in 16 cryomodules to accelerate the beam up to 800 MeV. The acceleration electric field is about 12.5 MV/m. Figure 4 shows the main-linac optics for acceleration and deceleration. Quadrupole triplets are placed at every two cryomodules for the beam focusing. The horizontal and vertical betatron functions are optimized against transverse beam break-up (BBU) due to the cavity HOMs.

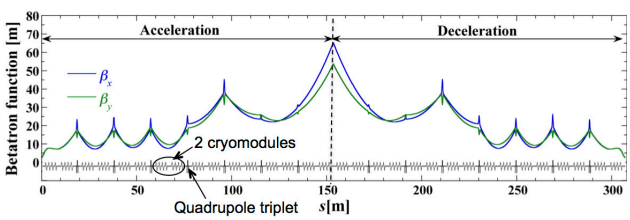

Figure 4: Horizontal and vertical betatron functions (β_x, β_y) of the main superconducting linac for the acceleration and deceleration phases.

HOM BBU and Heating

The BBU threshold current is calculated for the designed main-linac optics by using the simulation code *bi*[6]. The transverse HOM parameters of the Model-1 cavity are listed in Table 3. By scanning over the betatron phase and the return loop length, the minimum threshold current is calculated to be 195 mA without the HOM frequency randomization. It is well above the expected average current of the EUV source.

Table 3: HOM Parameters of the Model-1 Cavity

Frequency [GHz]	Q_e	R/Q [Ω/cm^2]	$(R/Q)\,Q_e/f$ [Ω/cm^2/GHz]
1.866	7732	6.43	26659
1.874	11655	8.77	54526
1.879	18360	1.95	19089
2.575	4899	21.32	40557
3.082	33608	0.98	10676

The HOM heating of the main-linac cavity should be considered. The parasitic loss of the beam is given by the following equation:

$$P_{loss} = k_{loss} Q_b^2 f \ . \qquad (1)$$

where the loss factor k_{loss} strongly depends on the bunch length. The parasitic loss is finally absorbed at the HOM damper. Therefore the maximum absorption power of the HOM damper restricts the bunch charge, length and frequency. Table 4 shows examples of estimated parasitic loss power for the Model-1 cavity. Our short-term target of the absorption power of the HOM damper is 30 W and the final goal is 100 W. In addition, the bunch frequency should be carefully selected so as to avoid heating resonant to monopole HOMs. Bunch frequencies of 130, 162.5, 260, 325 and 650 MHz are possible at least for the Model-1 cavity.

Table 4: Estimated Parasitic Loss of the Model-1 Cavity

Bunch length @cavity	**9.75mA x 2 60pC 162.5MHz**	**8mA x 2 100pC 81.25MHz**
1 ps	23.4 W	32 W
2 ps	17.6 W	24 W

FEL PARAMETERS

Here FEL parameters are briefly described. The FEL power P_{FEL} is roughly expressed by the product of the electron beam power $P_{electron}$ and Pierce parameter ρ_{FEL} as follows:

$$P_{FEL} = \rho_{FEL} P_{electron} \ . \qquad (2)$$

The electron beam power is the product of the beam energy E and the average beam current I_{av}. The Pierce parameter is given by

ISBN 978-3-95450-183-0

$$\rho_{FEL} = \left[\frac{1}{16} \frac{I_p}{I_A} \frac{K^2 [JJ]^2 \lambda_u^2}{\gamma^3 \sigma_x \sigma_y (2\pi)^2} \right]^{1/3}, \quad (3)$$

where I_p, I_A, γ, σ_x, σ_y, K and λ_u are the peak current, Alfven current(17kA), horizontal and vertical beam sizes, the K-vaue and magnetic period of the undulators. $[JJ]$ is $J_0[\xi]$-$J_1[\xi]$ with $\xi=K^2/(4+2K^2)$ for planar undulators and unity for helical undulators. The horizontal and vertical beam sizes are proportional to the square root of the horizontal and vertical emittances, respectively. High peak current and low emittance are important for the FEL power.

BUNCH COMPRESSION AND DECOMPRESSION SCHEME

Bunch compression is essential for achieving high peak current and decompression for efficient energy recovery without significant beam loss.

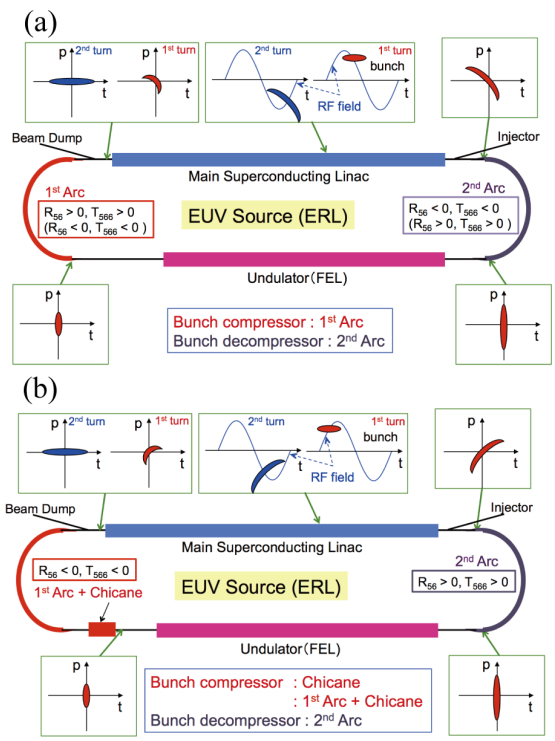

Figure 5: Bunch compression and decompression schemes: (a) The bunch compressor is the 1st arc. (b) The bunch compressor is only the chicane or combination of the 1st arc and chicane. For all the cases, the bunch decompressor is the 2nd arc.

The simplest scheme is that the bunch compressor is the 1st arc and the bunch decompressor the 2nd arc and illustrated in Fig. 5a. The 1st and 2nd arcs have the R_{56} and T_{566} values with different signs. The electron bunch from the injector is accelerated off crest in the main linac and compressed in the 1st arc with non-zero R_{56} optics. The sextupole magnets in the 1st arc optimize T_{566} in order to minimize the bunch length or maximize the Pierce parameter. The compressed bunch is used for the FEL in the long undulator section and then decompressed before the beam dump by using the optics of the 2nd arc and off-crest deceleration in the main linac.

Figure 5b shows two other bunch compression and decompression schemes using a chicane. One is that the bunch compressor is only the chicane and the other combination of the 1st arc and chicane. We try three different bunch compression schemes in our design study.

DESIGN OF ARCS AND CHICANE

Arc Sections

A 2-cell TBA lattice is used for design of the arc sections. Figure 6 shows the 2-cell TBA lattice and an example of the isochronous optics (R_{56}=0 m). The structure of the TBA cell is very similar to that of the cERL arcs. The bending radius and angle are 3 m and π/8 for each of the eight sector bending magnets. The lengths of the quadrupole and sextupole magnets are two times longer than that of the cERL because the beam energy is high. Optics matching of the two cells is done by four quadrupole magnets at the arc center. Eight sextupole magnets can be inserted in the arc to optimize T_{566}.

The R_{56} of the 2-cell TBA lattice is expressed with the bending radius ρ, the bending angle θ and the dispersion function η_c at the TBA-cell center as follows:

$$R_{56} = 4\rho(\theta - \sin\theta) + 2\eta_c \sin\theta . \quad (4)$$

The 2-cell TBA optics with different R_{56} values of ±0.3 m and ±0.6 m can be designed in a similarly way to the isochronous optics. The 2-cell TBA lattice has a wide dynamic range of R_{56}. The momentum acceptance is estimated from the maximum dispersion function to be more than 4% for a possible horizontal half-aperture of about 5 cm and expected to tolerate a large momentum spread caused by the FEL.

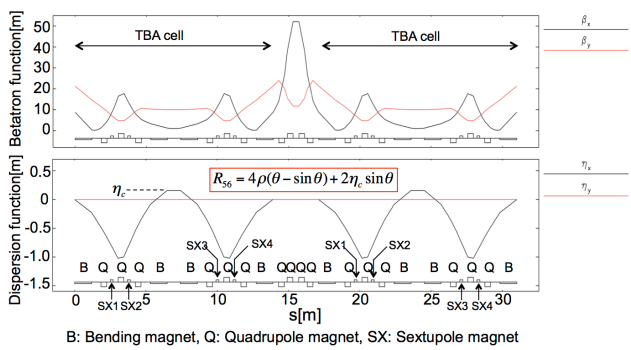

Figure 6: 2-cell TBA lattice and optics for the arcs. The betatron and dispersion functions of an isochronous optics (R_{56}=0 m) are shown in the upper and lower graphs.

ISBN 978-3-95450-183-0

Chicane

A chicane is designed with four rectangular bending magnets for the bunch compression. The R_{56} of this chicane is expressed by

$$R_{56} = -\frac{4L_B}{\cos\theta} - \frac{4L_B^2 L_D}{\rho^2 \cos^3\theta} + 4\rho\theta\,, \qquad (5)$$

where ρ, θ, L_B, and L_D are the bending radius, the bending angle and the magnet length and interval. In the design, the magnet length of 1 m and the magnet interval of 0.51 m are used. Figure 7a is chicane optics with R_{56} of -0.3 m for the bunch compression by only the chicane and Figure 7b chicane optics with R_{56} of -0.15 m for the bunch compression by combination of the 1st arc and chicane. They are used for the bunch compression simulations.

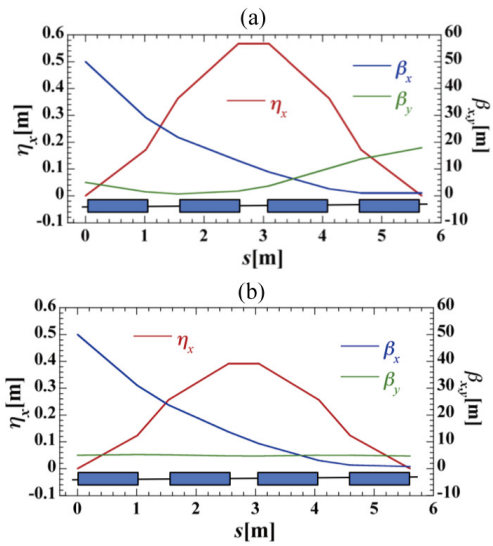

Figure 7: Dispersion function η_x and betatron functions (β_x, β_y) of the chicane for bunch compression (a) by only the chicane (R_{56}=-0.3 m) and (b) by the combination of the 1st arc and chicane (R_{56}=-0.15 m).

BUNCH COMPRESSION SIMULATION

The bunch compression simulation is performed for the three different schemes by using the simulation code *elegant*[7]. Figure 8 shows the simulation result of the bunch compression by the 1st arc, the chicane and their combination. In each of Figs. 8a to 8c, the upper graph shows optics from the entrance of the main linac to the exit of the 1st arc or the exit of the chicane. The 2-D longitudinal (time-momentum) distributions of the electron bunch at the entrance of the main linac, the entrance of the 1st arc and the exit of the 1st arc or the chicane are also shown. In the simulation, the initial distribution at the entrance of the main linac is assumed to be a 6-D Gaussian distribution with the injector parameter values estimated in the previous section. This is the case of the initial bunch length of 1ps and the bunch charge of 60 pC. The momentum spread is set to about 0.1 % after off-crest acceleration by the main linac.

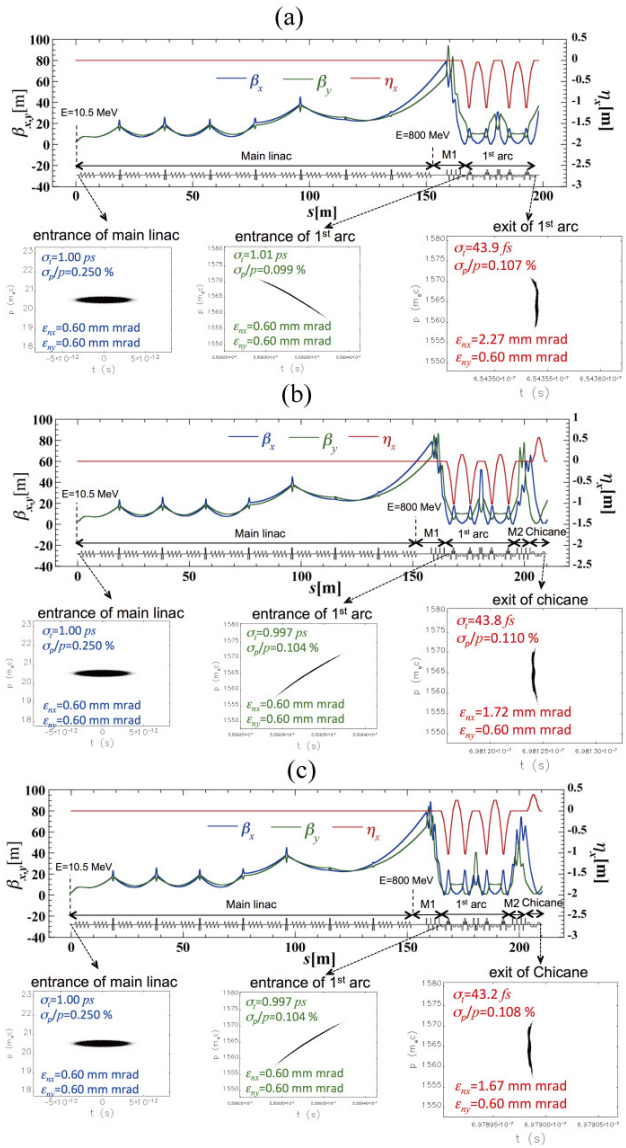

Figure 8: Optics from the main-linac entrance to the 1st arc exit or chicane exit and simulated time-momentum distributions at the main-linac entrance, the 1st arc entrance and the 1st arc exit or the chicane exit for the bunch compression by (a) the 1st arc, (b) the chicane and (c) their combination.

For the bunch compression by the 1st arc shown in Fig. 8a, the bunch length is compressed to about 44 fs by the 1st arc with R_{56}=0.3 m and the normalized horizontal and vertical emittances are 2.26 and 0.60 mm·mrad at the 1st arc exit. The normalized horizontal emittance is significantly increased by the CSR effects. In the case of the bunch compression by only the chicane in Fig. 8b, the 1st arc optics is isochronous (R_{56}=0 m) and the bunch is compressed by the chicane with the R_{56} value of -0.3 m. At the chicane exit after the bunch compression, the bunch length is almost the same as that of bunch

ISBN 978-3-95450-183-0

compression by the 1st arc. On the other hand, the normalized horizontal emittance is reduced to 1.72 mm·mrad because the CSR effects are reduced by optics adjustment described later. Figure 8c shows the simulation result of the bunch compression by combination of the 1st arc and chicane. Both the 1st arc and chicane have the same R_{56} value of -0.15 m. At the chicane exit, the bunch has almost the same parameter values as that of the bunch compression by only the chicane. The parameter values after the bunch compression are summarized in Table 5.

For the two bunch compression schemes using the chicane, the CSR-induced emittance growth is reduced by matching the phase ellipse angle to the CSR kick angle at the chicane exit, as shown in Fig. 9. The Pierce parameter becomes almost maximum at this matching condition. Such adjustment of the phase ellipse angle is found to be difficult for the bunch compression by the 1st arc having achromatic TBA optics with a fixed R_{56} value. Therefore the normalized horizontal emittance is large compared to those of the other two schemes using the chicane.

Table 5: Beam Parameters after Bunch Compression

Bunch Compressor	σ_t * [fs]	σ_p/p # [%]	ε_{nx}, ε_{ny} † [mm·mrad]
1st arc	43.9	0.107	2.27, 0.60
Chicane	43.8	0.110	1.72, 0.60
1st arc + Chicane	43.2	0.108	1.67, 0.60

* Bunch length # Momentum spread † Normalized horizontal and vertical emittances

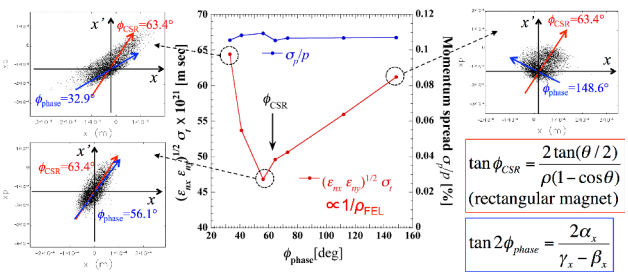

Figure 9: Maximization of the Pierce parameter by matching the phase ellipse angle ϕ_{phase} to the CSR kick angle ϕ_{CSR}=63.4 degrees. This is the case for the bunch compression by only the chicane at the bunch charge of 60 pC.

Figure 10 shows the peak current and normalized horizontal and vertical slice emittances in the bunch after the bunch compression for the three different bunch compression schemes. The slice emittances are more important for the FEL power than the projected ones listed in Table 5. The horizontal normalized slice emittance is lower at high slice peak currents than the projected one, especially for the two bunch compression schemes using the chicane.

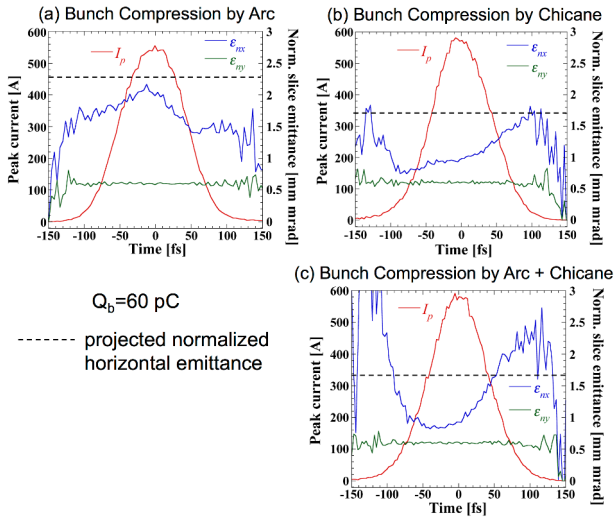

Figure 10: Peak current and normalized horizontal and vertical slice emittances in the bunch after the bunch compression for the three different bunch compression schemes. The broken line in each graph means the projected normalized horizontal emittance.

FEL PERFORMANCE

The FEL performance of the designed ERL-EUV source is calculated by using the FEL simulation code *Genesis*[8] and the simulation result of the bunch compression for the bunch charge of 60 pC. Helical undulators with the magnetic period of 28 mm are used for the FEL. Figure 11 shows the FEL pulse energy as function of the undulator section length, the FEL temporal profile and the FEL power spectrum for the bunch compression by combination of the 1st arc and chicane. The FEL pulse energy is 55.5 μJ without tapering and 67.6 μJ with 10% linear tapering at the undulator section length of 100 m. For the bunch frequency of 162.5/325 MHz, 9/18 kW FEL power is achieved at 9.75/19.5 mA without tapering and 11/22 kW at the same current with the 10% tapering.

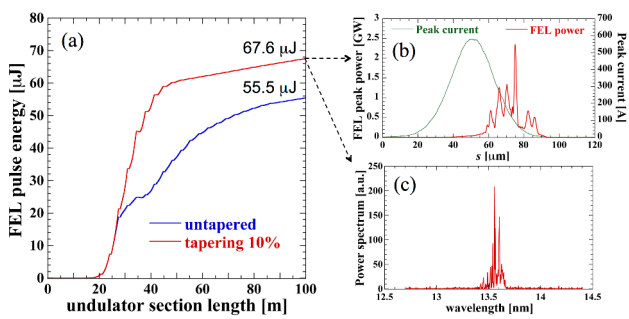

Figure 11: Calculated FEL performance of the designed ERL-based EUV source: (a) the FEL pulse energy as function of the undulator section length, (b) the FEL temporal profile and (c) the FEL power spectrum.

ISBN 978-3-95450-183-0

SUMMARY AND OUTLOOK

The design work on the ERL-based EUV source was recently started. The injector, main linac, arc sections and chicane have been designed. The bunch compression simulation has also been done. As a result, more than 10/20 kW FEL power is demonstrated at the average current of less than 10/20 mA. The present image of the designed EUV source is shown in Fig. 12. Further design work and optimization for the tapering, optics, beam and undulator parameters are expected to improve the FEL power. In addition, the bunch decompression simulation and finally S2E simulation from the gun to the beam dump should be performed.

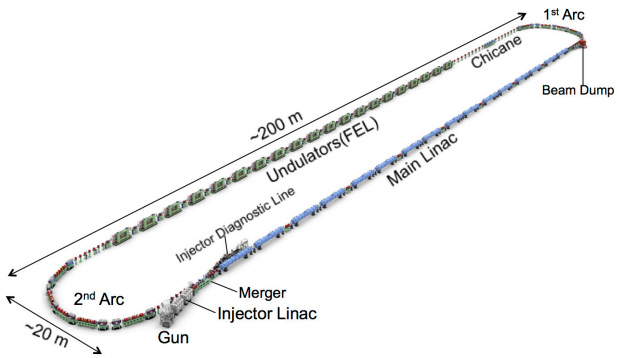

Figure 12: Present image of the designed ERL-based EUV source.

REFERENCES

[1] S. Sakanaka et al., MOPCTH07, ERL2015, Stony Brook, NY, USA.
[2] M. Yamamoto et al., TUIBLH1020, ERL2015, Stony Brook, NY, USA.
[3] *GPT*, http://www.pulsar.nl/gpt/index.html
[4] H. Sakai et al., WEIBLH2054, ERL2015, Stony Brook, NY, USA.
[5] H. Sakai et al., Proc. of ERL2007, Daresbury, UK, p.34 (2007).
[6] *bi*, http://www.lepp.cornell.edu/~ib38/bbu/
[7] *elegant*, http://www.aps.anl.gov/Accelerator_Systems_Division/Accelerator_Operations_Physics/manuals/elegant_latest/elegant.pdf
[8] *Genesis*, http://genesis.web.psi.ch

ISBN 978-3-95450-183-0